Mangrove Species Classification in Qi'ao Island Based on Gaofen-2 Image and UAV LiDAR

Yuchao Sun, Zheng Wei, Yang Gao, Hongkai Ren, Qidong Chen, Di Dong, and Ping Hu

Abstract Mangrove species classification is of great significance to the study of mangrove community structure and biodiversity. Most researches use foreign high-resolution remote sensing images or UAV images for mangrove species classification. In order to improve classification accuracy, LiDAR and hyper-spectral data are often used to assist classification. In this paper, based on the Gaofen-2 image and the CHM data obtained by the UAV Lidar, the mangroves in Qi'ao Island, Zhuhai are classified among species by using the random forest classification method. The classified species include 5 types of true mangroves, 3 types of semi mangroves, *Phragmites australis* and non-vegetation. The results show that the use of Gaofen-2 image can only effectively distinguish the *Sonneratia apetala*, *Acrostichum aureum* and non-vegetation, the accuracy of distinguishing other mangrove species is not ideal; After Gaofen-2 image fusion of CHM data, the classification accuracy of each mangrove species has been significantly improved, with the overall classification accuracy reaching 91.44%, which verifies the effectiveness of Gaofen-2 image fusion of external data in mangrove species classification research.

Keywords Mangroves · Qi'ao Island · Species classification · Gaofen-2 Image · CHM

Y. Sun · Z. Wei (✉) · Y. Gao · Q. Chen · D. Dong · P. Hu
South China Sea Institute of Planning and Environmental Research, State Oceanic Administration, Guangzhou 510300, China
e-mail: weizheng0628@foxmail.com

Key Laboratory of Marine Environmental Survey Technology and Application, Ministry of Natural Resources, Guangzhou 510300, China

H. Ren
Southern Marine Science and Engineering Guangdong Laboratory (Zhuhai), Zhuhai 519082, China

W. Wang et al. (eds.), *Communications, Signal Processing, and Systems*, Lecture Notes in Electrical Engineering 1032, https://doi.org/10.1007/978-981-99-7505-1_9

1 Introduction

Mangrove is a woody plant community that grows in intertidal zone of tropical and subtropical coast and is periodically submerged by seawater. It is an important coastal wetland ecosystem, and plays an important role in purifying seawater quality, protecting seawall, maintaining ecological balance and biodiversity [1, 2]. Due to the special habitat in the intertidal zone, field survey of mangrove is quite difficult. In recent years, remote sensing technology combined with field survey is commonly used to extract the mangrove distribution range [3], species classification [4] and biomass estimation [5, 6]. Mangrove species classification is of great significance to the study of mangrove community structure and biodiversity, but it also puts forward higher requirements for spectral resolution and spatial resolution of remote sensing images [7].

Mangrove species classification is mainly based on supervised classification methods, which carried out by combining the image spectral features from the band index and texture features [7]. While the spectral features were usually extracted from the band index and the texture features were from the gray level co-occurrence matrix. To improve the classification accuracy, many studies used hyperspectral images such as Gaofen-5 [8] and radar images such as RADARSAT-2 [9] or combined multiple types of remote sensing image data to carry out mangrove species classification [10]. With the wide application of unmanned aerial vehicle (UAV), more and more UAV remote sensing data are also applied to the mangrove species classification. Using the light detection and ranging (LiDAR) to assist the UAV orthophoto image can effectively improve the accuracy of classification [11, 12]. The combination of mangrove canopy height model (CHM) extracted from UAV Lidar and UAV hyperspectral images can also improve the classification accuracy [13].

In the past decade, most of the data sources used for mangrove species classification are mainly foreign high-resolution images, which with high cost. In recent years, domestic high-resolution images such as Gaofen series and Ziyuan series have been gradually applied to various applications due to their high resolution and low cost, and have also been applied to the mangrove species classification [14]. However, due to the small number of spectral bands and other reasons, it is difficult to obtain ideal classification accuracy. To improve the classification accuracy of domestic high-resolution images, this paper takes the mangrove reserve of Qi'ao Island in Zhuhai as an example, fuses the Gaofen-2 image with the UAV LiDAR data and discusses the adaptability of the domestic high-resolution image in mangrove species classification.

2 Study Area and Data Sets

2.1 Study Area

Qi'ao Island is in the northeast of Zhuhai city and on the west bank of the Pearl River Estuary, covering an area of about 24 km^2. It has a subtropical monsoon climate, with an annual average temperature of 24.5 °C, the lowest temperature in January and the highest temperature in July. The average annual sunshine hours can reach 1907.4 h, the average annual precipitation is about 1964.4 mm, mainly concentrated in April to September, and the average annual relative humidity of the air is about 79%. The tide in this area is irregular semidiurnal tide, and the annual average value of seawater salinity is 18.4 ‰, belonging to the coastal saline meadow marsh soil.

According to the field survey, the mangroves of Qi'ao Island are mainly distributed in the northwest and west of Qi'ao Island (Fig. 1). There are 10 families, 13 genera and 15 species of true mangroves in Qi'ao Island, mainly composed of *Sonneratia apetala* (SA), *Acrostichum aureum* (AA), *Acanthus ilicifolius* (AI), *Kandelia candel* (KC) and *Aegiceras corniculatum* (AC), among which SA community is the absolute dominant community. There are 7 families, 9 genera and 9 species of semi-mangroves, mainly including *Heritiera littoralis* (HL), *Bruguiera gymnorrhiza* (BG, mainly refer to seedling of BG) and *Hibiscus tiliaceus* (HT). In addition, there are many reeds (RE) associated with mangrove growing areas [15, 16]. According to the field survey and measurement, there are obvious differences in the height of mangrove species (Table 1), and the distribution of mangroves is characterized by clustering in species [17].

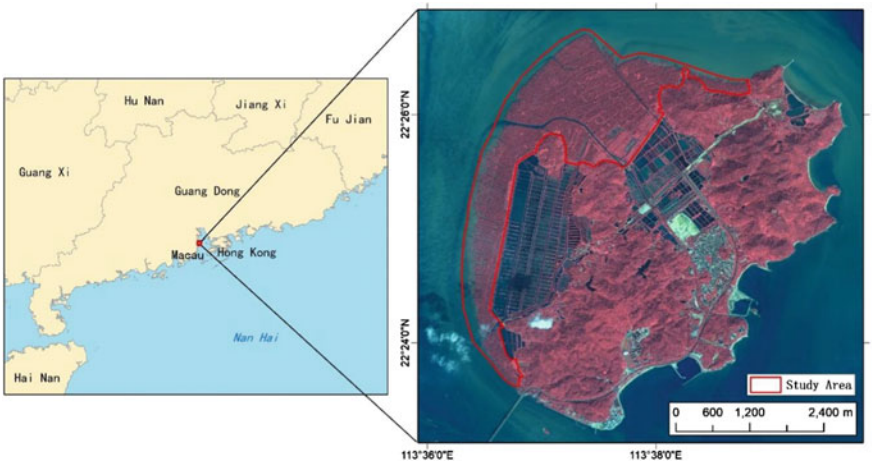

Fig. 1 Location of Qi'ao island and region of study area

Table 1 Height of different mangrove species

Species	SA	AA	AI	KC	AC	HL	BG	HT	RE
Height (m)	10–20	1–2	1–2	3–5	2–3	6–10	2–3	6–8	1–2

2.2 Data Sets

2.2.1 Gaofen-2 Image

Gaofen-2 satellite is the first civil optical remote sensing satellite with a spatial resolution better than 1 m independently developed by China, which was launched in August 2014. Gaofen-2 carries two high-resolution spectral sensors: 1 m panchromatic and 4 m multispectral cameras, has the characteristics of high radiation accuracy, high positioning accuracy and rapid attitude mobility. Gaofen-2 images are widely used in natural resource survey, agricultural crop yield estimation, water conservancy flood facilities and disaster monitoring [18, 19].

We obtained the Level-1A product of Gaofen-2 image on November 1, 2021, which covers the whole Qi'ao Island. We used ENVI 5.3 software for radiometric calibration, and the "FLAASH Atmospheric Correction" tool for atmospheric correction, the 30 m resolution DEM data released by the National Aeronautics and Space Administration (NASA) in February 2020 was used for orthophoto correction, and the "Gram-Schmidt Pan Sharpening" tool was used for image fusion to obtain an image with a resolution of 1 m and four multispectral bands.

2.2.2 UAV LiDAR Data

The UAV Lidar data is obtained by Shenzhen FEIMA V10 UAV system with DV-LiDAR20 airborne laser. The FEIMA V10 UAV has a length of about 175 cm, a wingspan of 415 cm, a takeoff weight of 25 kg, a maximum load of 6 kg, a cruise speed of 20 m/s, a endurance time of about 160 min (6 kg load), a wind resistance level of 6, a standard configuration of network RTK/PKK and its integrated solution service (Fig. 2a). The FEIMA DV-LiDAR20 laser system weighs about 3.5 kg and has a size of 216 mm × 384 mm × 166 mm, the maximum range is 1350 m, the wavelength is 1550 nm, and the transmission frequency is 50–550 kHz, which integrates a 42 megapixel full-frame camera with a focal length of 18 mm (Fig. 2b).

The Lidar data was obtained in November 17, 2021, the flight altitude was 300 m, and the elevation accuracy was about 7 cm. We used FEIMA "UAV Manager" and LiDAR360 Software for pre-processing, used "denoising" tool for point cloud denoising, used "classification" tool for ground point and vegetation point classification, exported digital elevation model (DEM) with a resolution of 1 m based on ground point, and digital surface model (DSM) with the same resolution based on vegetation point, canopy height model (CHM) was calculated by difference between DSM and DEM.

(a) FEIMA V10 UAV (b) FEIMA DV-LiDAR20

Fig. 2 FEIMA UAV LiDAR system

2.2.3 Mangrove Species Data

To understand the distribution characteristics of mangrove species in Qi'ao island and collect the sample data, a field survey was carried out in December 10, 2021. We mainly used camera and GPS to take photos of different mangrove species and record their coordinates. We established position and mangrove species association based on GPS data and remote sensing image (Fig. 3).

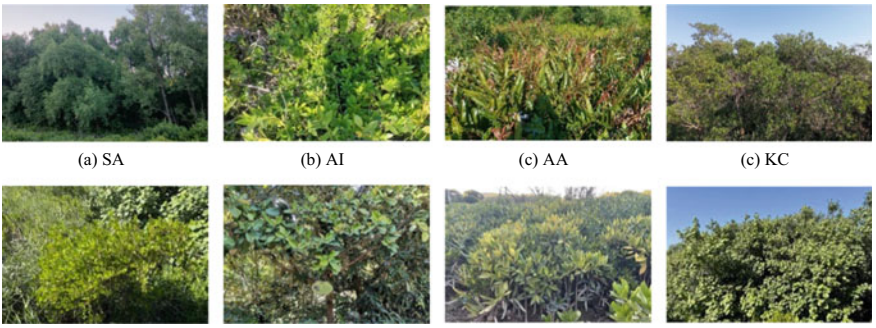

(a) SA (b) AI (c) AA (c) KC

(e) AC (f) HL (g) BG (h) HT

Fig. 3 Photos of different mangrove species in Qi'ao island

3 Methods

3.1 Mangrove Species Samples Selection

According to the field photos and GPS data, we established remote sensing interpretation marks of different mangrove species based on the GaoFen-2 image, and selected sample points data for different mangrove species on the GaoFen-2 image (Table 2). Non-vegetation (NV) refers to water, bare ground and artificial buildings, half of the samples data are used as training data and half as validation data.

3.2 Random Forest Classification

There are many algorithms applied to mangrove species classification, including support vector machine (Ting Wang et al., 2015), random forest [8, 9] and other supervised classification methods [20] based on pixel or object-oriented. Among them, the RF algorithm proposed by Breiman [21], has been proved to have high prediction accuracy, good tolerance for outliers and noise, and is not prone to overfitting [22], which is widely used in mangrove and other vegetation classification [23]. The RF algorithm is an ensemble algorithm for supervised classification based on classification and regression trees (CART). By combining the characteristics of CART, bootstrap aggregating, and random feature selection, independent predictions can be established and therefore improve accuracy.

Before RF classification, we used object-oriented method to segment and merge GaoFen-2 image in ENVI 5.3 software. Through experiments, we got the best object-oriented segmentation effect when the segmentation threshold is 60 and the merge threshold is 20. RF classification was also carried out in ENVI 5.3 software after segmentation, we selected the training data in Sect. 3.1 as sample data, the number of trees was set to 100, the number of features was set to square root, the impurity function was set to Gini coefficient.

Table 2 Mangrove species samples data

Species	SA	AA	AI	KC	AC	HL	BG	HT	RE	NV	Total
Training data	55	20	20	20	15	20	20	20	30	40	260
Validation data	55	20	20	20	15	20	20	20	30	40	260

3.3 Mangrove Species Classification Based on GaoFen-2 Image

We conducted the object-oriented RF classification for GaoFen-2 image using the method in Sect. 3.2. Considering the rich texture information in GaoFen-2 image and large texture difference among mangrove species [24], we extracted the texture features by calculating Grey Level Co-occurrence Matrix (GLCM) for blue band (Band3) of GaoFen-2 image [25]. The GLCM parameter included mean, variance, homogeneity, contrast, dissimilarity, entropy, angular second moment and correlation. By combining the GLCM bands with the spectral bands of GaoFen-2 image, the object-oriented RF method was used for classification.

3.4 Mangrove Species Classification Based on GaoFen-2 and CHM

Due to the high spatial resolution and less spectral band, GaoFen-2 image combined with hyperspectral images, synthetic aperture radar (SAR) images or LiDAR should be adopted to achieve more accurate classification results [26]. Considering the obvious differences of tree height among mangrove species in Qi'ao Island, which can be reflected in the CHM data of LiDAR, the combination of GaoFen-2 image (including GLCM) and CHM data should effectively improve the classification accuracy. The object-oriented RF classification was also applied to combined data.

3.5 Accuracy Assessment

Confusion matrix is used to evaluate the classification accuracy. The evaluation indicators of confusion matrix include Overall Accuracy (OA), Kappa coefficient (Kappa), Producer Accuracy (PA) and User Accuracy (UA). OA represents the proportion of the number of correctly classified samples to the total number of samples; Kappa reflects the consistency between classification results and reference samples; PA represents the proportion of the number of samples correctly classified to the total number of reference samples; UA represents the proportion of the number of samples correctly classified to the total number of true samples.

4 Results and Discussion

4.1 Results

The object-oriented RF method was adopted to classify the GaoFen-2 image, GaoFen-2 + GLCM data and GaoFen-2 + GLCM + CHM data refer to Sects. 3.2–3.5. The validation data in Sect. 3.1 was used to calculate the classification accuracy (Table 3).

4.2 Discussion

Texture information and CHM data can effectively improve the classification accuracy of GaoFen-2 image according Table 3, By fusing texture information and CHM data, the OA of GaoFen-2 image reached 84.88% from 74.50%. From Table 4, using the spectral band of GaoFen-2 image can distinguish SA, BG and NV (whose PA and UA are both above 70%) due to the spectral difference of mangrove species. By comparing Tables 4 and 5, the PA and UA of AA, KC and PA are obviously improved after fusing texture information due to the textural difference of mangrove species. By comparing Tables 5 and 6, the PA and UA of AI, HL and HT have greatly

Table 3 Classification accuracy of different GaoFen-2 image

Input data	OA (%)	Kappa	Confusion matrix
GaoFen-2 image	74.50	0.7103	Table 4
GaoFen-2 + GLCM	80.92	0.783	Table 5
GaoFen-2 + GLCM + CHM	84.88	0.8278	Table 6

Table 4 Confusion matrix of GaoFen-2 image

%	SA	AA	AI	KC	AC	HL	BG	HT	RE	NV	PA	UA
SA	90.85	1.13	0	4.68	0	5.56	0	0.56	6.3	0	90.85	92.16
AA	0	63.28	1.69	0	0	2.78	1.67	0	5.93	0	63.28	80.58
AI	0	0	61.02	0	0	7.22	5.56	26.11	5.93	0	61.02	55.67
KC	5.49	0	0	91.81	42.22	10	1.67	3.33	0	0	91.81	58.58
AC	1.42	28.81	0	1.75	52.59	16.11	0	0.56	5.19	0	52.59	40.34
HL	0	0	0	0.58	0.74	41.67	5	0.56	11.85	0	41.67	63.03
BG	0	0	20.34	0	0	0	81.11	8.89	0	0	81.11	73.74
HT	0	0	3.95	0	1.48	5.56	4.44	45	0.74	0	45	73.64
RE	2.24	6.78	12.99	1.17	2.96	11.11	0.56	15	64.07	0	64.07	63.37
NV	0	0	0	0	0	0	0	0	0	100	100	100

Table 5 Confusion matrix of GaoFen-2 + GLCM data

%	SA	AA	AI	KC	AC	HL	BG	HT	RE	NV	PA	UA
SA	95.93	0	0	8.77	0	4.44	0	0	3.33	0	95.93	93.65
AA	0	71.75	1.69	0	0	0	0	0	1.48	0	71.75	94.78
AI	0	0	69.49	0	0	0	14.44	13.89	10	0	69.49	61.19
KC	1.02	2.82	0	71.93	21.48	0	1.67	3.33	0	0	71.93	71.93
AC	0	7.91	0	14.04	66.67	12.78	0	0.56	2.22	0	66.67	56.96
HL	3.05	7.34	0	4.68	6.67	66.67	0	12.22	3.33	0	66.67	61.22
BG	0	0	12.43	0	0	4.44	78.33	0	0	0	78.33	82.46
HT	0	0	12.43	0	0	11.11	0	70	6.67	0	70	67.74
RE	0	10.17	3.95	0.58	5.19	0.56	5.56	0	72.96	0	72.96	81.74
NV	0	0	0	0	0	0	0	0	0	100	100	100

Table 6 Confusion matrix of GaoFen-2 + GLCM + CHM data

%	SA	AA	AI	KC	AC	HL	BG	HT	RE	NV	PA	UA
SA	97.97	0	0	10.53	0	2.78	0	0	3.33	0	97.97	93.77
AA	0	71.75	0	0	0	0	0	0	0.37	0	71.75	99.22
AI	0	0	75.71	0	0	0	11.11	7.78	10.37	0	75.71	68.37
KC	0.41	1.69	0	74.85	13.33	1.11	0	1.67	0	0	74.85	82.05
AC	0	15.25	0	9.94	71.11	0.56	1.67	0	3.33	0	71.11	62.75
HL	1.22	1.13	0	4.09	6.67	82.78	0	13.33	1.48	0	82.78	74.13
BG	0	0	14.69	0	0	4.44	81.67	0	0	0	81.67	81.22
HT	0	0	2.82	0	0	8.33	0	77.22	3.7	0	77.22	82.25
RE	0	10.17	6.78	0.58	8.89	0	5.56	0	77.41	0	77.41	79.77
NV	0.41	0	0	0	0	0	0	0	0	100	100	99.45

improved after fusing CHM data due to the height difference of mangrove species. Take HL as an example, parts of HL are confused with SA, AA and RE by using the spectral and texture information of GaoFen-2 image, the discrimination is improved after fusing CHM data.

Although fusing texture information or CHM data can improve the overall accuracy and PA/UA of most mangrove species, there is also a reduction in the accuracy of individual mangrove species. Take KC in Tables 4 and 5 as an example, the PA reduces from 91.81 to 71.93% after fusing texture information, this may be caused by the lack of universality of KC validation sample selection. Similar situation appears in AC of Tables 5 and 6, the proportion of AA wrongly classified into AC increased from 7.91 to 15.25%, which decreased from 28.81 to 15.25% in Tables 4 and 5 due to the large difference in texture, while the similar height of AA and AC increases the difficulty of distinguishing between the two types of mangrove species, which also increases the proportion of wrongly classification after fusing CHM data.

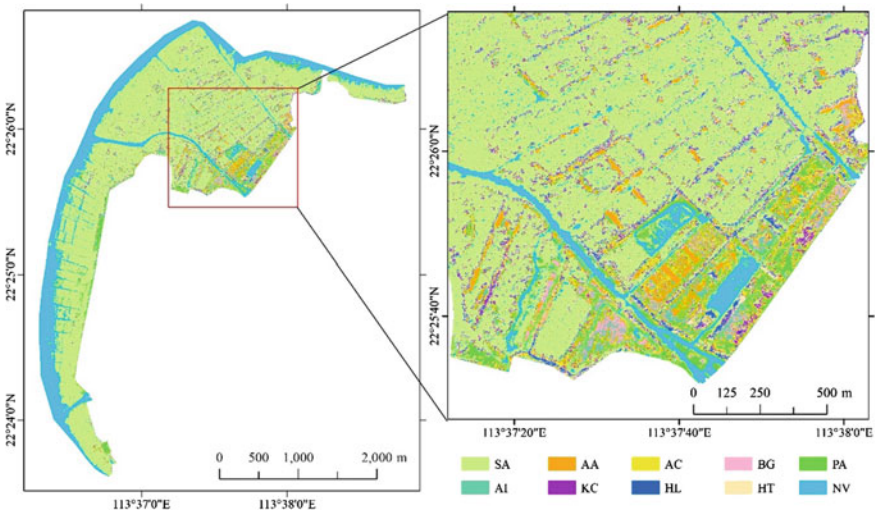

Fig. 4 Map of mangrove species in Qi'ao Island

4.3 Mapping

We use the best classification result for mapping, the classification result of GaoFen-2 + GLCM + CHM was converted into vector and mapped by ArcGIS (Fig. 4). From Fig. 4, SA has the widest distribution area among the mangrove species in Qi'ao Island, which distributed throughout the study area. AI, AA and RE are distributed between SA, while KC, AC, HL, BG, and HT are mainly distributed in the southeast of the study area and is relatively concentrated.

5 Conclusions

In this paper, the mangrove reserve of Qi'ao Island in Zhuhai is taken as the study area, and the UAV CHM data is fused with the GaoFen-2 image to classify the mangrove species. The research results show that due to the lack of spectral bands, Gaofen-2 image cannot better identify mangrove species other than AC and BG. After fusing textural information from GaoFen-2 image and CHM data from UAV LiDAR, the classification accuracy of mangrove species is significantly improved. The main achievements of this study are as follows:

(1) The spatial resolution of GaoFen-2 image up to 1 m provides the possibility of mangrove species classification. Due to its small number of bands, it cannot reflect the spectral differences between different mangrove species well, nor

can it achieve high classification accuracy. However, the abundant texture information contained in the GaoFen-2 image plays a good auxiliary role in distinguishing different mangrove species and can greatly improve the classification accuracy.

(2) Although the fusion of texture information can effectively improve the classification accuracy of the GaoFen-2 image, the accuracy for mangrove species classification is still unsatisfactory. The CHM data obtained by UAV LiDAR can well reflect the difference between mangrove tree heights, and can further improve the accuracy of mangrove classification after being fused with the GaoFen-2 image. The experiment shows that the Gaofen-2 image combined with external CHM data can meet the requirements of mangrove species classification, and can achieve reasonable classification accuracy.

Acknowledgements This research was supported by Independently setting up projects of Key Laboratory of Marine Environmental Survey Technology and Application, Ministry of Natural Resources (MESTA-2021-C005; MESTA-2022-C002); Key Program of Marine Economy Development Special Foundation of Department of Natural Resources of Guangdong Province (GDNRC [2022]19).

References

1. Giri C, Ochieng E et al (2011) Status and distribution of mangrove forests of the world using earth observation satellite data. Global Ecol Biogeogr
2. Katherine E, Robert T, Jin O (1998) Different kinds of mangrove forests provide different goods and services. Glob Ecol Biogeogr Lett 7(1):83–94
3. Deng G (2002) Application of remote sensing technology in mangrove resources investigation. Central South Forest Invent Plan 01:27–28
4. Liu K, Li X, Wang S, Zhong K, Qian J (2005) Monitoring of the changes of mangrove wetland around the Zhujiang Estuary in the past two decades by remote sensing. Trop Geogr 2005(02):111–116
5. Wang Y (2018) Estimation of mangrove biomass in Shenzhen Bay based on multi-source remote sensing data. Southwest University
6. Xu F (2020) mangrove extraction and carbon storage estimation by using Sentinel-2 images. Lanzhou Jiaotong University
7. Li S (2012) Mangroves spatial distribution extraction and species discrimination based on remote sensing data in Beibu Gulf. Nanjing University
8. Wan L, Lin Y, Zhang H, Wang F, Liu M, Lin H (2020) GF-5 Hyperspectral data for species mapping of mangrove in Mai Po. Hong Kong Remote Sens 12:656
9. Zhang H, Wang T, Liu M, Jia M, Lin H, Chu LM, Devlin AT (2018) Potential of combining optical and dual polarimetric SAR data for improving mangrove species discrimination using rotation forest. Remote Sens 10(3):467
10. Ferrentino E, Nunziata F, Zhang H et al (2020) On the ability of PolSAR measurements to discriminate among mangrove species [J]. IEEE J Sel Top Appl Earth Observ Remote Sens 13:2729–2737
11. Liu K, Gong H, Cao J, Zhu Y (2019) Comparison of mangrove remote sensing classification based on multi-type UAV data. Tropical Geography 39(4):492–501

12. Liu X, Bo Y (2015) Object-based crop species classification based on the combination of airborne hyperspectral images and LiDAR data. Remote Sensing 7(1):922–950
13. Cao J, Liu K, Zhuo L, Liu L, Zhu Y, Peng L (20121) Combining UAV-based hyperspectral and LiDAR data for mangrove species classification using the rotation forest algorithm. Int J Appl Earth Observ Geoinform 102(1):1569–8432
14. Li X, Liu K, Zhu Y et al (2018) Study on mangrove species classification based on ZY-3 image. Remote Sens Technol Appl 33(2):360–369
15. Qiu N, Xu S, Qiu P et al (2019) Community distribution and landscape pattern of the mangrove on the Qi'ao Island, Zhuhai. Scientia Silvae Sinicae 55(1):1–10
16. Zhen W, Weijun C, Wei G et al (2017) Study on Zhuhai Qi'ao island main mangrove community characteristics. J Central South Univ Forest Technol 37(4):86–91
17. Hu Y, Zhu N, Liao B et al (2019) Carbon density and carbon fixation rate of mangroves of different restoration types in Qi'ao island. J Central South Univ Forest Technol 39(12):101–107
18. Cao W, Wang W, Wang X et al (2021) Research on crop classification based on GF-2 satellite. Geomatics Spat Inform Technol 44(04):158–161
19. Wu D, Yu W, Xie T (2020) Application of GF-2 satellite data for monitoring organic pollution delivered to water bodies in the Guangdong-Hong Kong-Macao Greater Bay Area. Trop Geogr 40(4):675–683
20. Dezhi W, Bo W, Penghua Q, Yanjun S, Qinghua G, Xincai W (2018) Artificial mangrove species mapping using Pléiades-1: an evaluation of pixel-based and object-based classifications with selected machine learning algorithms. Remote Sens 10:294
21. Breiman L (2001) Random forests. Mach Learn 45(1):5–32
22. Zhao LJ, Tang P (2016) Scalability analysis of typical remote sensing data classification methods: a case of remote sensing image scene. J Remote Sens 20(2):157–171
23. Wang W, Dong Z, Fu D et al (2020) Classification of mangrove in Leizhou Bay based on ZY-3. Hydrogr Survey Chart 40(01):35–39
24. Huang X, Zhang L, Wang L (2009) Evaluation of morphological texture features for mangrove forest mapping and species discrimination using multispectral IKONOS imagery. IEEE Geosci Remote Sens Lett 6:393–397
25. Rao CN, Sastry SS, Mallika K, Tiong HS, Mahalakshmi KB (2013) Co-occurrence matrix and its statistical features as an approach for identification of phase transitions of mesogens. Int J Innov Res Sci Eng Technol 2:4531–4538
26. Peng L, Liu K, Cao J, Zhu Y, Li F, Liu L (2020) Combining GF-2 and RapidEye satellite data for mapping mangrove species using ensemble machine-learning methods. Int J Remote Sens 41(3):813–838